

conductivity and the gap conductance data provided in NEACRP benchmark specification for a Westinghouse three-loop plant.

2.3. Pinwise calculations

The 2D/1D diffusion FDM solver taking each pin-cell as the base mesh was employed. Errors originating from the diffusion theory and the coarse mesh size were simultaneously corrected by the superhomogenization (SPH) factor, as well as the errors from the pin-level homogenization and the group condensation.

The transient calculation was performed with the Crank-Nicolson method and the time step size was set to 0.005 sec. The fuel and moderator models are briefly shown in Table I. In test calculations, it was observed that the effective fuel temperature (T_{eff}) model provided in Ref. [4] (TF1) leads to inconsistencies in the thermal feedback effect. Therefore, another model in Ref. [6] (TF2) was additionally used. The TF2 model corrects the volume-weighted average temperature (\bar{T}_f) of the fuel by difference between the pellet centerline temperature (T_c) and the surface temperature (T_s).

Table I. Fuel and moderator model for the pinwise calculation

Effective fuel temperature	TF1: $T_{eff} = \omega T_c + (1 - \omega) T_s$, $\omega = 0.3$
	TF2: $T_{eff} = \bar{T}_f - \frac{1}{18} (T_c - T_s)$
Gap conductance	Function of linear power density
Heat transfer coefficient	Dittus-Boelter
Total active core flow	15849.4 kg/s

3. Results

3.1. Steady state hot zero power core cases

The hot zero power (HZIP) core calculations aimed to check the consistency of core models for the two codes. The steady state calculations were performed for two cases, one with the all regulating rods are inserted (ARI) and the other with the ejected rod (N-1). The critical boron concentration (CBC) was searched for the ARI case and the k-eigenvalue calculation was performed for the N-1 case with the CBC of the ARI case to predict the static rod worth of the ejected rod.

Table II and III briefly show the result, and Fig. 2 shows the reference radial power and the assembly ΔP (%) distributions of the N-1 core. The results were highly satisfactory in respect that the no notable deterioration of the agreement was observed in between the ARI and the N-1 cases, although the ejection of the rod lead to severe skewness of the power distribution. Peaking factor (Fr, Fxy, and Fq) predictions were also matched well.

It is worth noting that quite large pin power errors were observed in the fresh MOX assemblies, because the MOX PXSs obtained from the single lattice contains errors originating from differences in the flux spectra. The result shows the need for application of an improved homogenization technique to improve the accuracy of the pinwise calculation for MOX loaded cores.

Table II. Results of the HZIP ARI core calculation

		KARMA	Pinwise	Diff.
CBC (ppm)		1246.3	1263.3	17.0 ppm
Peaking Factor	Fr	1.893	1.890	-0.13%
	Fxy	1.896	1.891	-0.26%
	Fq	2.843	2.841	-0.08%
Assembly 2D ΔP (%)			RMS	0.82%
			MAX	2.56%
Pinwise 2D ΔP (%)			RMS	1.20%
			MAX	-6.22%
Pinwise 3D ΔP (%)			RMS	1.22%
			MAX	-6.89%

Table III. Results of the HZIP N-1 core calculation

		KARMA	Pinwise	Diff.
Reactivity (pcm)		647.5	642.2	-5.3 pcm
Peaking Factor	Fr	6.133	5.989	-2.35%
	Fxy	6.161	5.997	-2.67%
	Fq	9.211	9.000	-2.29%
Assembly 2D ΔP (%)			RMS	0.81%
			MAX	2.53%
Pinwise 2D ΔP (%)			RMS	1.19%
			MAX	-6.25%
Pinwise 3D ΔP (%)			RMS	1.20%
			MAX	-6.91%

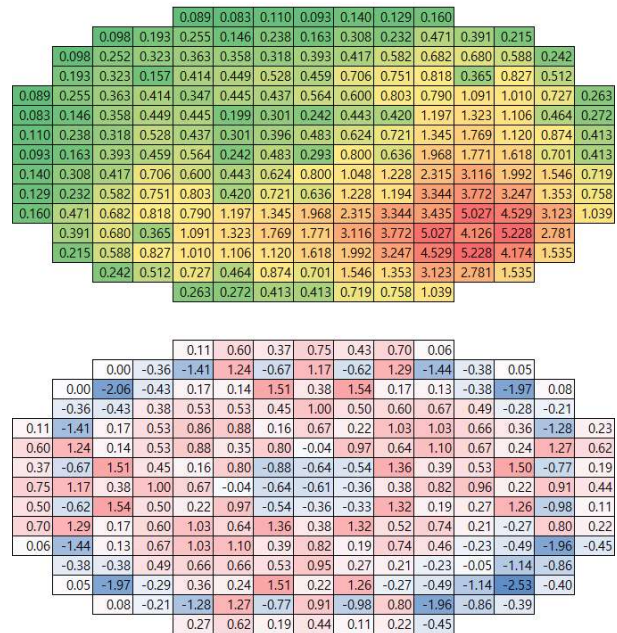


Fig. 2. Assembly-wise radial power (top, KARMA) and ΔP (%) distributions of the N-1 core

3.2. Transient rod ejection case

The results are summarized in Table IV. The peak time predicted by the pinwise calculation shows only 0.005 sec difference with the reference, and the difference of the peak power is 5.9% with TF1 and -4.5% with TF2. This satisfactory result clearly verifies the reliability of transient module implemented in the pinwise code.

Table IV. Results of the transient rod ejection case

	Peak time (sec)		Peak power (%)	
	Value	Error	Value	Error
KARMA	0.275	-	226.0	-
Pinwise, TF1	0.280	0.005	239.2	5.9
Pinwise, TF2	0.280	0.005	215.7	-4.5

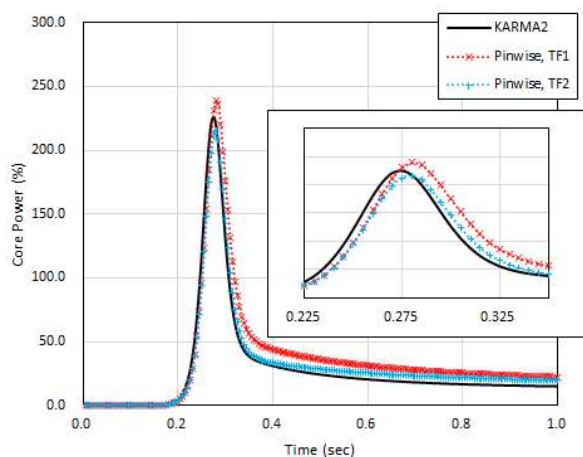


Fig. 3. Transient core power behavior

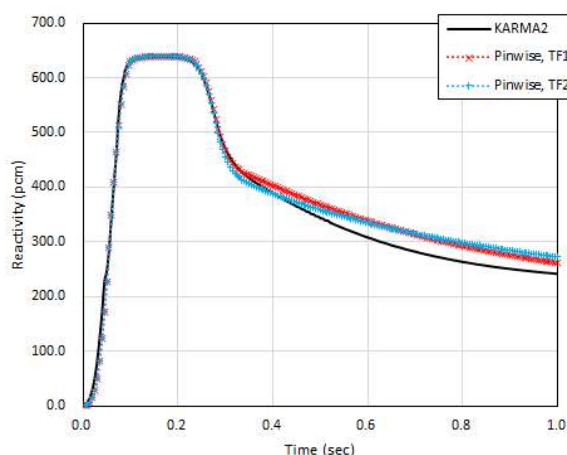


Fig. 4. Transient core reactivity behavior

The difference originating from the fuel temperature models becomes notable after 0.3 sec. The core power behavior in Fig. 3 and the reactivity behavior in Fig. 4 indicate that the fuel temperature feedback is stronger with the TF2 model, especially at the rear end of the

power peak. It leads to the core power behavior matches better with the reference.

4. Conclusion

Transient module of the pinwise core calculation code was successfully verified through the consistent code-to-code comparison. Comparing with the reference DWCC solution yielded by KARMA, the 8-group pinwise core calculation accurately predicted the core power behavior. Difference of the peak time was only about 0.005 sec, and that of the peak power was less than 5.9% and 4.5% with the different fuel temperature models.

In future works, various energy group structures will be employed, and more extensive problems will be used for not only the verification but also the validation of the pinwise core calculation code.

REFERENCES

- [1] J. I. Yoon et al., "Verification & Validation of KARMA/ASTRA with Benchmark and Core-Follow Analyses", *Trans. ANS*, Washington D.C., USA, Oct. 30 – Nov. 3, 2011 (2011).
- [2] H. Yu et al., "Application of Modified 2D/1D Decoupling Method in the Pin-wise Core Analysis", *Trans. KNS*, Jeju, Korea, May 18 – 19, 2023 (2023).
- [3] H. Hong et al., "Preliminary Assessment for Improved Features of KARMA Lattice Transport Code through PWR Core Follow Calculations", *Trans. ANS*, Phoenix, Arizona, USA, Nov. 13 – 17, 2022 (2022).
- [4] T. Kozłowski, T. Downar, "PWR MOX/UO₂ Core Transient Benchmark, Final Report", NEA/NSC/DOC(2006)20, OECD NEA, 2006.
- [5] J. Kang, "Enhancement of Direct Whole Core Transient Calculation Capability", PhD Thesis, Seoul National University (2022).
- [6] D. Bernard et al., "LWR-UO_x Doppler Reactivity Coefficient: Best Estimation Plus (nuclear and atomic sources of) Uncertainties", *Procs. M&C2017*, Jeju, Korea, April 16 – 20, 2017 (2017).